This is the accepted version of the paper.

This version of the publication may differ from the final published version.

Permanent repository link: https://openaccess.city.ac.uk/id/eprint/18332/

Link to published version: https://doi.org/10.1016/j.jcsr.2017.09.029

Capacity of semi-rigid composite joints in accommodating column loss

Shan Gao[a,b], Lanhui Guo[b*], Feng Fu[c], Sumei Zhang[b]

[a] School of Civil Engineering, Xijing University, Xian 710000, China

[b] School of Civil Engineering, Harbin Institute of Technology, Harbin 150090, China

[c] Department of Civil Engineering, City University London, London, EC1V0HB, UK

Abstract: In the scenario of column loss, joints would be subjected to bending moment combined with a tensile force due to large vertical displacement, where tensile force plays a critical role in resisting progressive collapse of structure by providing the catenary force. In order to study the effect of tensile force on the behavior of semi-rigid composite joints in structures in the case of column loss, six semi-rigid flush- endplate connections tests were conducted, which include pure flexural tests, pure tensile tests and combined flexural and tensile tests. The experimental results indicate that under pure bending moment condition, the semi-rigid composite joint displays sufficient rotation capacity for forming "catenary action". It is characteristic of the semi-rigid composite joint that its moment capacity decreases in a linear manner together with the increase of tensile load. Also, the capacity of semi-rigid composite joints is compared with that of the full-welded rigid composite joints. The tensile strength of high-strength bolts would not exert any effect on the initial stiffness of semi-rigid joint, but bring about decline in the moment resistance and tensile resistance of semi-rigid joint. The joints tend to fail at "catenary phase" under tensile force. A simplified $M\text{-}N$ correlation formula for composite joint is proposed to describe the behavior of joint in structures under column loss. The finite element model with material failure criterion can predict the fracture of bolt in semi-rigid composite joint.

Keywords: composite joints; progressive collapse; bending moment combined with tension; semi-rigid

1. Introduction

Nowadays, the events of terrorism are on the trend of increase. Public buildings such as hospital, shopping mall and car parks, whose collapse would lead to catastrophic results, turn vulnerable to terrorist attacks. Normally the abnormal loads caused by terrorist attacks such as bomb explosion, fire or vehicle impact are not explicitly taken into account in design. These abnormal loads may result in a significant local loss to load-carrying capacity of

critical columns and subsequently to the collapse of the whole building. To prevent this type of failure, the alternate load path method is recommended in design [1-3] which is checked through the performance evaluation of the remaining structure in the removal of a critical column. The load-carrying mechanisms of the remaining structure will change from plastic hinge action to tensile catenary action where the beam-column connection is subjected to the combination of bending moment and tensile force as shown in Fig.1.

In order to avoid brittle damages of joint and behave properly, the joint should possess enough redundancy and ductility. Therefore, the features of joint behavior are identified as follows: under plastic hinge action, the reverse load-carrying capacity of the joint is required in where the joints at the damaged column are under sagging moment rather than under hogging moment; During the transition of load-carrying mechanism, the joints at the damaged column and the adjacent columns should be capable of carrying the particular load sequences involving bending moments, axial forces and shear forces; After tensile catenary action is triggered on the beams, the joints would undergo large deformation without any significant reduction in strength. The development of large deformations, as locally usual in the damaged structure is accepted, as long as progressive collapse is prevented [4]. There features are seldom to encounter in conventional design but essential for preventing progressive collapse in structure under column loss.

Steel-composite structures are widely used in the construction of public buildings. Commonly steel beams are acting compositely with the concrete slab. Compared with bare steel joints, steel-concrete composite joints possess higher bearing capacity and initial stiffness, especially higher redundancy which is a critical feature of joints employed in design of preventing progressive collapse. Moreover the reinforcement in the slab of composite joint is a key component of "catenary action", especially when the steel joint fails to meet the rotation demand to activate "catenary action". According to the joint's rotational stiffness, a joint may be classified as rigid, nominally pinned or semi-rigid. In reality, there is no real fully rigid joint. For an example, even the full rigid designed joint will exhibit some rotations in real engineering project. According to EC3, if the rotational stiffness of the joint is over a special value, the joint can be assumed as rigid joint. Compared with simply supported joints, semi-rigid or rigid joints intended to sustain bending moments may display comparatively enhanced behavior [5]. Due to the relatively complicated configuration, however, semi-rigid joints are not widely used in public building structures even though semi-rigid joints can optimize the bending moment distribution in the connected beams. And above all, semi-rigid joints possess good rotation capacity which is especially beneficial for activating "catenary action" in the system in preventing progressive collapse.

It is common for the component method from Eurocode 3 to describe the behavior of steel-concrete composite joints. The mechanical properties of any beam-column connection could be estimated through decomposing it into individual components sustaining a specific action [5]. Based on the principles of component method, experimental and theoretical studies have been performed [6-9] to investigate the moment resistance, initial stiffness and rotation capacity of composite joints. Although the rules of component method theoretically work on any combination of actions, only 5% of axial resistance of the supported beam is allowed to apply on the joint in the Eurocode 3. However the joints in the structures under abnormal loads may withstand great axial force which may exceed the limits. Hence several experimental and theoretical studies have been conducted on the development of the component method to take a substantial axial load into consideration [10-13]. It should be noted that the focus of those researches was on development of the component method, rather than on description of the behavior of the joints in progressive collapse.

Based on that concept, a European collaborative research project [14] was set up to study the robustness of steel-concrete composite frame. In particular, a series of experiments was conducted on the behavior of composite frame in the scenario of column removal while an analytical method intended to predict M-N (bending moment-axial force) resistance interaction curves for composite joints was proposed based on the results of the experiments. Guo [15-17] also conducted a series of researches on the performance of steel-concrete frame under column removal. Five rigid composite joints employed in the frames were tested under bending moment in combination with tension. The experimental results indicated that the bending resistance of rigid composite joint decreases linearly with the increase of tension. Stylianidis and Nethercot [5] developed a mechanical model for evaluating the behaviour of steel and composite joints used in anti-collapse analysis.

As can be seen from the aforementioned literatures, the previous studies on composite joints mainly focused on the moment resistance, initial stiffness and rotation capacity under conventional loading conditions. Up to date, few experiments have been conducted on the capacity of semi-rigid composite joints in accommodating accidental loss of adjacent structural members, especially the action of combined bending moment with tensile force. In this paper, tests were conducted on a series of flush endplate semi-rigid composite joints in the scenario of column removal. The loading conditions involve pure bending, pure tension and the combination of bending moment and tension in the tests. The mechanical performance of flush endplate composite joints in the scenario of column loss was studied first in detail and then compared with the studies on rigid composite joints. Moreover, a finite element model based on material failure was developed by ABAQUS software [18] and validated against the experimental results.

2. Experimental program

2.1. Design and fabrication of specimen

According to the loading capacity of actuator and experimental set-up, six 1/3-scale specimens of steel-concrete composite joints were designed and fabricated, whose parameters are presented in Table 1. The material properties and dimensions of the joints are identical as those of the joints employed in the semi-rigid composite frame in Ref. [17]. The configuration of flush endplate connection was employed in the specimens as shown in Fig. 2. Grade 10.9 M16 high-strength bolts were adopted in all specimens except that Grade 8.8 M16 high-strength bolts were adopted in specimen SJST2. The profile sections of beam and column were H200×100×5.5×8 (H-overall depth(d)× flange width(b_f)×web thickness(t_w)×flange thickness(t_f)) and H200×200×8×12 respectively. The thickness of the endplate was 12 mm. Detailed dimensions of the bare steel specimens are shown in Fig. 3.

The depth and width of reinforced concrete (RC) slab were 100 mm and 800 mm respectively. Along the length of the RC slab, two layers of 12-mm-diameter bars were utilized as longitudinal reinforcements beside the column. The longitudinal reinforcements in the middle of the rebar mesh were cut off at the location of beam-column connection. The longitudinal reinforcement ratio of the slab was 0.85%. Transverse reinforcements of 8 mm were distributed in two layers in the RC slab, as shown in Fig. 4. The16-mm-diameter studs with spacing of 100 mm were welded onto the steel beam, thereby achieving full shear interaction which means there is no relative movement between RC slab and steel-beam before composite beam reaches its moment capacity. The yield stress of studs was 235MPa.

The structural steel of Grade Q235 and HPB235 were adopted for steel members and rebars respectively. Grade 10.9 and Grade 8.8 bolts were used to connect steel beam and steel column. The results of the material tests are listed in Table 2, where f_y, f_u, and E_s stand respectively for yield stress, tensile strength and elastic modulus of structural steel. Casting work of concrete was conducted in the lab of Harbin Institute of Technology with the specimen located at the test position. Both the 150×150×150 mm cubes and 150×150×300 mm cylinders were tested for strength and Young's modulus of concrete respectively at the same time. The average compressive strength of concrete is 26.2 MPa whilst the Young's modulus of concrete is 2.65×10^4 MPa.

2.2. Experimental setup

As shown in Fig. 5 (see Ref. [19] for more details), the specimens of semi-rigid joints were tested in the

multifunctional loading ring, the same as the specimens of rigid joints in Ref. [15]. With this loading ring, moment and tensile force could be applied onto the joints simultaneously which is not easy to achieve by means of common experimental facility. The details of the experimental setup are illustrated in Fig. 6.

For specimen SJS, SJH and SJT which sustained bending moment or tensile force only, the vertical load was regarded as the controlling criteria in elastic range. After the specimen yielded, the loading method of displacement control was used until the joint failed to carry loads.

As the previous experimental and theoretical researches related to progressive collapse analysis showed, four main stages would be gone through by the frame structure under column loss, namely elastic stage, elastic-plastic stage, transient stage and catenary phase. In the first two stages, the additional loads are mainly sustained by the moment resistance of the joint, while the axial force is considerably low in the joint. In the transient stage, the load-bearing mechanism of frame is in the state of transition from "plastic hinge action" to "catenary action". The axial load would increase in this stage. After the frame has gone into the catenary phase, "plastic hinge action" has faded due to the loss of moment capacity in the joint [17].

Based on these observations and assumptions, the SJST and SJHT tests were conducted to study the behavior of the joint in the transient stage. The considerably low axial force in the elastic stage and elastic-plastic stage is assumed to be neglected at Step A. And then tensional force was applied at Step B to simulate the transition from "plastic hinge action" to "catenary action". For specimen SJST, SJST2 and SJHT which sustained combined bending moment and tensile force, the load was applied through two steps as shown in Fig. 7:

Step A: Apply vertical load onto the top of column. Through applying vertical load, a bending moment is first applied on the specimen. The vertical jack would be arrested and hold constantly after the plastic yield moment of the joint is reached which is determined by corresponding pure bending tests. It should be noted that the beam-ends should rotate freely while the vertical load is applied in order to keep additional tensile force from occurring to the beam.

Step B: Apply horizontal tensile force at both ends of beam. While the rotation of the joint is kept a constant value, the ends of the beams are continuously loaded until the joint fails. As shown in Fig. 8, tension rod (⑦) is screwed into bolt sleeve (⑧) to transfer the tensile load applied by horizontal jack to the specimen. By connecting the beam-ends to bolt sleeve (⑧) with a pivot shaft, the boundary condition of simply-supported is realized while tensile load is applied.

Linear variable displacement transducers (LVDTs) were distributed to measure the vertical and horizontal displacements of the specimens. The distribution of LVDTs is presented in Fig. 9. The following values were measured: vertical displacement of column and beams (LVDT1-LVDT3), axial deformation of composite beams (LVDT4 and LVDT5), and displacements at support (LVDT6 and LVDT7).

3. Experimental phenomena

3.1. Specimen SJS

Specimen SJS was tested under a sagging moment. Specimen SJS remained elastic in initial behavior without showing any evident phenomenon. The first crack on the slab, initiated at the tip of the column flange as shown in Fig. 10(a), was observed at 100 kN. When the load increased to 180 kN, crush of concrete was observed beside the flanges of column as shown in Fig. 10 (b). Displacement loading method was adopted subsequently. With the increase of displacement, the vertical load decreased slightly. At the displacement of 100 mm, with a loud sound, one of the bolts at the left connection was fractured and ejected. The test was brought to a termination. As shown in Fig. 10(c), the endplate deformed dramatically. The column flange showed no evidence of deformation. The cracking pattern on the top surface of slab was presented in Fig. 10(d). It can be seen that the concrete near the web of column was crushed and peeled off. Cracks at RC slab of SJS were intensively distributed around the column. The failure mode of specimen SJS was the fracture of bolts.

It is worthy to notice that the cracking pattern of semi-rigid joints under sagging moment was different from that of the fully-welded rigid joints which were comparative specimens with the same configuration except beam-to-column connection in Ref. [15]. In the test of Ref. [15], the longitudinal cleavage cracks at the top surface of RC slab were distributed directly over the steel beam. The same cracks were not observed in this test. With the majority deformation of the semi-rigid joint from the beam-to-column connection, there was a relatively small displacement between steel beam and slab. It may be concluded that the adoption of semi-rigid beam-to-column connection would help to release the longitudinal shear force between slab and steel beam.

3.2. Specimen SJST, SJST2

Specimen SJST and SJST2 were tested under a combination of sagging moment and tensile force. M16 bolts with 10.9 Grade were used in beam-to-column connections of specimen SJST while 8.8 Grade M16 bolts were used in specimen SJST2, in which M16 means the diameter of bolt is 16 mm.

In the bending step A, the vertical load was applied onto the column. Initially, specimen SJST remained elastic without any evident phenomenon. The first crack on the bottom-surface of RC slab, as occurred at 120 kN, initiated at the tip of the column flange. When the load reached 165 kN, the yield load was reached and step A was finished. At this stage of loading, there were a few slight cracks on both sides of the slab.

And then by restraining the vertical displacement, tensile loads were applied on both beam-ends of the joint. Under tensile load of 350 kN, the transverse cracks were propagated through the whole length of the RC slab. Under the tensile load of 1000 kN, four bolts of the left beam-to-column connection were fractured in tension, which also proclaimed the termination of the test, as shown in Fig. 11(a). The final cracking pattern of top surface of RC slab was shown in Fig. 11(b). Two main cracks besides the flange of column were obviously observed due to the deformation of endplate. Welding seams between endplate and beam flange on right side of the connection were fractured as shown in Fig. 11(c). The failure mode of specimen SJST was the fracture of bolts and welding seams.

The experimental phenomenon of specimen SJST2 with 8.8 Grade M16 bolts was similar with the specimen SJST. The simple bending test corresponding to specimen SJST2 was not conducted. Tensile force was applied when the stiffness of vertical force-displacement curve decreased remarkably. The final cracking pattern on the top surface of RC slab was shown in Fig. 12(a). Two main cracks were also observed beside the flanges of column. The test was terminated due to the fracture of bolts at 900 kN. The failure mode of specimen SJST2 was the fracture of bolts and welding seams as shown in Fig. 12(b).

It is worthy to notice that the cracking pattern of the semi-rigid joints in Fig. 11 and Fig. 12 was completely different from the cracking pattern of the rigid joints in Fig. 13 in Ref. [15]. As the rotational stiffness and tensile stiffness of semi-rigid joints were smaller than those of the beam, so was the deformation focused on the beam-column connection rather than on composite beams. This difference was also observed in the tests of composite frames with the same rigid and semi-rigid joints in Ref. [16] and Ref. [17].

3.3. Specimen SJH

Specimen SJH was tested under a hogging moment. Specimen SJH initially showed signs of elasticity in behavior without any evident phenomenon. The first crack on the top surface of RC slab, as initiated at the tip of the

column flange as shown in Fig. 14(a), occurred at 30 kN. Buckling of bottom flange of steel beam appeared at at 150 kN when displacement loading method was adopted. Vertical load decreased when the displacement reached 40 mm. At the displacement of 180 mm, specimen SJH was no longer able to carry loads when the test was terminated. As shown in Fig. 14(b), severely buckling occurred at bottom flanges and webs of steel beam. No gap was observed between the endplate and column flange. Cracking pattern on the top of slab was shown in Fig. 14(c), which was similar to that of specimen with fully-welded connection in Ref. [15]. The failure mode of specimen SJH was the buckling of steel beam.

3.4. Specimen SJHT

Specimen SJHT was tested under a combination of hogging moment and tensile force. At first, specimen SJHT remained elastic in behavior, without any evident phenomenon during step A under the state of bending. The first cracks on the top surface of RC slab, as initiated at the tip of the column flange occurred at 50kN. Slight buckling occurred at bottom flange of steel beam at 150 kN when tensile force was applied. Two main cracks formed beside the flanges of column. As the tensile load increased, the amount of cracks at the bottom of slab increased evidently. When the tensile load reached 1000 kN, the welding seam between endplate and beam flange fractured as shown in Fig. 15(a). Consequently the test was terminated. The final cracking pattern on the top surface of slab was shown in Fig. 15(b). From the comparison between the experimental phenomena in the tests of specimens SJST and SJHT, it could be concluded that the failure mode of the joints under the combination of bending moment and tensile force depended on the level of internal force in the bolts.

3.5. Specimen SJT

Specimen SJT was tested under tensile forces. When the tensile force increased to 100 kN, the cracks occurred and spread over the top and bottom of the slab. As shown in Fig. 16(a), a 1-mm gap was observed at the end of the endplate under the tensile load of 750 kN. When the tensile load increased to 950 kN, the test had to be terminated because the welding seams between endplate and steel beam fractured as shown in Fig. 16(b). The bending deformation of bottom end of the endplate was greater than that of top end of the endplate. The cracking pattern at the top of the slab is shown in Fig. 16(c). Two main transverse cracks near the column flanges were observed which means the deformation of the joint under tensile force concentrated on the beam-to-column connections.

4. Experimental results and discussions

4.1. Relationship between bending moment and rotation

Fig. 17 shows the bending moment-rotation curves of specimen sustained bending moment. The legends of RJS and RJH represent the experimental results of rigid composite joints in Ref. [15] where RJS and RJH mean the rigid joint under sagging-moment and hogging-moment respectively.

The sagging moment resistance of specimen SJS is 119 kN.m, which is 1.3 times of the hogging moment resistance of specimen SJH (91 kN.m), as shown in Fig. 17. Specimens SJS and specimen SJH are close in initial stiffness to each other. From comparison between the experimental results of rigid composites in Fig. 17, it can be seen that the behavior of specimens SJH and RJH are similar under hogging moment. It indicates that the configuration of flush endplate would decrease the moment resistance and initial stiffness of composite joint under sagging moment compared to the joints under hogging moment. When semi-rigid joint is under hogging moment, as shown in Fig. 18, the behavior of the joint depends on tensile component and compressive component, which are the rebar in the RC slab and bottom flange of steel beam, respectively. Therefore specimens SJH and RJH are with similar behavior.

The rotation in response to the ultimate resistance is defined as ultimate rotation. It can be seen that the ultimate rotation of specimen SJH is similar to that of specimen RJH. The reason is that the buckling at the bottom flange results in the decrease of rotation capacity when the joint is subjected to hogging moment. It is worthy to notice that both the joints with rigid connection and semi-rigid connection meet the rotation demand for "catenary action" [3] of 0.02 rad. The experimental results of composite frame in Ref. [16-17] show that the deformation ability of composite frame under column loss mostly depends on the rotation capacity of the joints above the damaged column. It indicates that theoretically semi-rigid joints which possess good rotation capacity should be adopted for connecting beams to critical columns in case that "catenary action" needs to be activated to carry abnormal loads.

4.2. Relationship between bending moment and tensile force

The bending moment-rotation relations of specimen SJST and specimen SJHT in loading step A are shown in Fig. 19(a). Compared with the results of pure bending test, a good match forms between the curves of the pair composed of SJS and SJST, and the pair composed of SJH and SJHT. As described above, tensile force was applied

at the beam-ends after the joints have yielded which would result in additional moment to joints. The moment of the joints is given as follows:

$$M = P / 2 \cdot L - N \cdot \Delta \qquad (1)$$

where P stands for the vertical load applied on the column; L is the length of beam; N is the tensile force; Δ is the vertical displacement of the column; and M is the bending moment.

Fig. 19(b) shows the bending moment-tensile force relations of specimen SJST and specimen SJHT. It can be seen that the bending moment of the joints assumes a linear decline along with the increase of tensile force. After the tensile force was applied onto specimen SJST, the internal force on the RC slab gradually changed from compression to tension. And then RC slab would crack and fail to work. The rebar in RC slab would participate in bearing tensile force with steel beam together. The final state of specimen SJST would be similar to that of specimen SJHT. It suggests that the bending moment-tensile force curves of specimen SJST and specimen SJHT intersect with each other at a point.

An envelop curve consisting of two bending moment-tensile force curves would be obtained. The points sitting on the envelop curve present the plastic behavior of semi-rigid composite joints under combined bending moment and tensile load. In this state, the load-carrying mechanism of the joint is transforming from "plastic-hinge action" to "catenary action" when a tensile force begins to increase in the plastic hinge of the joint and decrease the moment resistance and rotation capacity of the joint. In addition to rotation capacity, the redundancy of the joint should be adequate to finish this transition. It means that every component of composite joint should act properly during the transition. If any component of the joint fails to work, there should be spare components to redistribute the internal force to avoid the progressive failure of the joint.

Also, Fig. 19(b) shows that the tensile load of 900 kN is attained at the intersection point whereas the bending moment is not equal to 0. This can be explained by the fact that the reference point used to compute the applied bending moment does not correspond to the tensile center of the joint. Hence there is an extra moment applied by tensile load when the moment applied by vertical load decreases to zero.

4.3. Relationship between tensile force and deformation

Fig. 20 presents the behavior of specimen SJT under bare tensile force. The plastic tensile resistance of the joint observed from the curve is 950 kN, which is approximately equal to the tensile load at intersection point A in Fig. 19(b). It confirms that the envelop curve in Fig. 19(b) could serve to describe the plastic state of the joint under

combined bending moment and tensile load. The ultimate tensile resistance of joint is 1060 kN which is 1.1 times of the plastic tensile resistance. And the ultimate axial deformation is 4 times of the plastic axial deformation. Through the comparison between the results of tensile test in Ref. [15], it indicates that the tensile behavior of this flush-endplate semi-rigid composite joint is not as good as that of fully-welded rigid composite joint. That is because that the deformation of the flush endplate leads to the fracture of welding seam as shown in Fig. 21. Meanwhile, the high-strength bolts which act as a tensile component in the beam-to-column connection are with low ductility. Particular attention should be given on the development of joint ductility and redundancy under tensile load.

4.4. Influence of bolt strength

Fig. 22(a) presents the bending moment-rotation relations of specimens SJST and SJST2 in step A. It is worthy to notice that before yield moment is reached, two specimens are similar in behavior, and their initial stiffnesses are almost the same. Along with the increase of sagging moment, a gradual balance of pre-tension is achieved in bolts (85 kN for 8.8M bolts and 110 kN for 10.9M bolts). When the pre-tension in 8.8M bolts goes to zero, the correspondent moment at the joint calculated by hand is about 32 kN.m. As seen from Fig. 22(a), at the moment of 30 kN.m, the stiffness of specimen SJST2 begins to get lower than that of specimen SJST. Fig. 22(b) shows the bending moment-tensile force curves in step B. By using 8.8M16 bolts in specimen SJST2, it is possible to decrease the moment resistance and tensile resistance of semi-rigid joint, but impossible to change the linear relationship between moment resistance and tensile resistance. Under proper design, Grade 10.9 and 8.8 bolts both could ensure the transition of load-carrying mechanism from "plastic-hinge action" to "catenary action". It is still suggested that Grade 10.9 bolts are adopted in flush endplate connection to improve the performance of the joint under combined bending moment and tensile force.

4.5. Behavior of semi-rigid joints in structures under column loss

As shown in Fig. 23, the load-carrying mechanism of the frame with semi-rigid connections in the scenario of middle column removal is composed of six phases [17]. Along with the progress of vertical deformation of damaged column, Joint A and Joint B in Fig. 23(a) are under the loading conditions involving pure bending, bending combined with tension and pure tension. The semi-rigid composite joints with the same configuration in the frame were tested herein under these loading conditions. The experimental results help to verify the detailed behavior of the frame under middle column removal and establish a relation between vertical load P and deformation Δ.

Before transient phase, the frame carries the vertical load through "plastic hinge action" which refers to the moment resistance of Joint A and Joint B. Without considering "compressive arch action", the relationship between P and Δ could be expressed as:

$$P = f(\Delta) \tag{2}$$

which involves the moment resisatnce and rotation stiffness of joint as studied above.

"Compressive arch action" is caused by the non coincidence of rotational centers of the connections under sagging and hogging moment as shown in Fig. 24. Although "arch phase" is defined to follow "elastci-plastic phase", compressive arch action is activated along with application of the vertical load. By restraining the deformation of endplate, compressive arch action helps the joint reach relatively high moment resistance and rotation stiffness.

During transient phase, the joints sustain the bending moment coupled with a tensile load. Along with the increase of vertical deformation, the tensile force would increase as the bending moment decreases to zero. In this phase, the relationship between P and Δ depends on the load-carrying mechanism transition between " plastic hinge action" and "catenary action". In this case, the relationship between between P and Δ could be expressed as:

$$P = f(\Delta, M, N) \tag{3}$$

where the relationship between M and N could be obtained from the tests in this paper while N could be explicitly expressed in Δ .

As presented in Fig. 25, various loading combination may be detected during the different phases as demonstrated in Fig. 23. Before transient phase (from point O to point C), the joints are under bending moment coupled with compressive load due to compressive arch action. And then the bending moment decreases along with the increase of tensile load. The segment of C(D)-E in Fig. 25 is studied through the aforementioned test. Based on the experimental results herein, the joints tend to fail at "catenary phase" under tensile load. Hence it is worthy to pay attention to the deformation capacity and resistance of semi-rigid joint under tensile load. More studies should be carried on in the future.

5. Numerical analysis

5.1. Finite element modeling

A finite element (FE) model is developed to validate against the experimental results by ABAQUS [18]. Solid elements (C3D8R) are adopted to simulate the steel beam, steel column, bolts and RC slab. Truss elements (T3D2)

are adopted to perform the behavior of rebar which are embedded into the slab. *Tie command is used to achieve the composite action between steel beams and concrete slab. The pre-tension of bolt in the simulation are applied as the same value as the experimental test. *Predefined field command from ABAUQS library is adopted to simulate the pre-tension in bolt.

The FE model is shown in Fig. 26. Only 1/2 of model is modeled, due to the symmetry of the specimens and experimental setup. The material properties and dimensions are identical to those of the specimens. The stress-strain relationships of material are as shown in Fig. 27. A bi-linear relationship with stress hardening is employed as both compressive and tensile stress-strain relation of steel. The stress-strain relationships of concrete in Chinese Code for Design of Concrete Structures (GB 50010-2010) are introduced into ABAQUS. Ten percent of compressive strength and the value of 0.5 MPa are regarded as tensile strength and remaining strength in tension of concrete respectively. Meanwhile, the plastic behavior of concrete is simulated by the Concrete Damage Plasticity model in ABAQUS library.

5.2. Model validation and result analysis

Only the loading condition of combined bending moment and tensile force is simulated herein. The loading procedure adopted into the simulation is the same as that in the tests. As shown in Fig. 28, the results based on the FE model matches well with the test results. The moment decreases linearly as the tensile force increases, with the location of the interaction point unchanged.

According to the numerical results and test results, a simplified *M-N* correlation formula could be derived as follows:

$$\frac{M}{M_p} + \frac{N}{N_p} = 1 \tag{4}$$

where M_p and N_p stand respectively for plastic moment resistance and plastic tensile resistance of the joint.

The plastic moment resistance M_p and plastic tensile resistance N_p of composite joint could be calculated by using "component method". Therefore *M* or *N* in Eq. (3) could be substituted by using Eq. (4). And then the relationship of vertical load *P* and vertical deformation Δ in "transient phase" would be explicitly described. More details about the relationship of *P* and Δ could be seen in Ref. [20].

5.3. Bolt fracture modeling

The failure modes of all six specimens are listed in Table 3. The failure of the specimens is due to the fracture of both bolts and welding seam. When the joint is subjected to hogging moment, the bolts in the connection are under low-level internal force and the welding seam between steel beam and endplate is the weakest part in the connection. When the joint is subjected to sagging moment or pure tensile force, the bolts are under high-level tensile internal force, and the resistance of the joint depends on the resistance of bolts or the welding seam. However, the welding seam between steel beam and endplate is supposed to possess the same strength as the beam section which means the welding seam should not fracture before the bolts in the connection. In practice, the failure of the welding seam may occur at any phase and, theoretically speaking, may be far from predictable. On the contrary, the fracture of bolts could be avoided by design. Thus it is necessary to develop a model to predict bolt fracture.

In order to simulate bolt fracture, a material fracture criterion in ABAQUS is employed. Once the fracture strain of bolt is attained, the element would be deleted from the model. As aforementioned, the fracture of bolts mostly appears in the catenary phase,thus only the loading condition of pure tensile load (specimen SJT) is simulated to validate the model.

Fig. 29 presents the final deformation of the joint under tensile load. As shown in Fig. 29(c), after fracture of the two bolts indentified in the bottom bolt rows, the deformation modes of the FE model are similar to the observed experimental deformation. And meanwhile, although the fracture of bolts at bottom rows results in the failure of FE model, as could be seen from Fig. 29(d), the juction between beam web and endplate is under high level of Von Mises stress, in which case it tends to fail.

Fig. 30 shows the development of bolt fracture. Due to the deformation of endplate, the fracture of the bolt initiates at the position of endplate. The final fracture mode of bolt model is similar to that of the bolt in specimen SJST as shown in Fig. 30(f). It indicates that the FE model with the help of material fracture criterion could simulate the initiation and evolution of bolt fracture.

Fig. 31 shows the comparision between experimental results and numerical results. The results of test and FE model match well in initial stiffness and yield strength. The failure mode of FE model is the fracture of bolts while that of specimen SJT is the fracture of welding seam between steel beam and endplate. In that case, the ultimate tensile deformation of FE model is larger than that of specimen SJT. In practice, the premature failure brought by welding seam fracture should be avoided due to its unpredictablity while the fracture of bolts should also be kept under control.

6. Conclusions

Six semi-rigid flush-endplate connections were tested. The tests involve three loading conditions, namely pure bending moment, bending moment combined with tensile load and pure tensile load. A study is made on the behavior of semi-rigid composite joints in structures under column removal. A finite element model with material fracture criterion is developed to simulate connection failure. The following conclusions can be made:

1. Under pure bending moment, semi-rigid composite joint possesses good rotation capacity which meets the needs of forming "catenary action". Under hogging moment, the behavior of semi-rigid composite joint is similar to that of rigid composite joint.

2. The moment capacity of composite joint decreases linearly along with the increase of tensile force. The points sitting on the M-N envelop curve present the plastic behavior of semi-rigid composite joint during the transition of load-carrying mechanism.

3. The tensile behavior of this flush-endplate semi-rigid composite joint is not as good as that of fully-welded rigid composite joint. Low strength bolts, as used in flush endplate connection, would not influence the initial stiffness of semi-rigid joint, but reduce the moment resistance and tensile resistance of semi-rigid joint.

4. Before transient phase, the joints are under bending moment combined with compressive load due to compressive arch action. Based on the experimental results, the joints tend to fail at "catenary phase" under tensile load.

5. Based on experimental and numerical analysis, a simplified M-N correlation formula for composite joint is proposed to describe the behavior of joint in structures under column loss. A finite element model with material failure criterion is developed to predict the fracture of bolt in semi-rigid composite joint.

Acknowledgements

References

[1]   Office of the Deputy Prime Minister. The Building Regulations 2000, Part A, Schedule 1:A3, Disproportionate Collapse, London, UK, 2004.

[2]   United States General Services Administration (GSA). Progressive collapse analysis and design guidelines for new federal office buildings and major modernization projects. Washington (DC). 2003.

[3]   U.S. Department of Defense. Unified Facilities Criteria: Design of Building to Resist Progressive Collapse [S]. UFC 4-023-03, USA, 2013.

[4]   Haremza C., Satiago A., Demonceau J.F., Jaspart J.P., Simoes da Silva L. Composite joints under M-N at elevated temperatures [J]. Journal of Constructional Steel Research. 2016, 124:173-186.

[5]   Stylianidis P.M., Nethercot D.A. Modelling of connection behaviour for progressive collapse analysis [J]. Journal of Constructional Steel Research. 2015,113:169-184.

[6]   Xiao Y., Choo B.S., Nethercot D.A. Composite connections in steel and concrete. Ⅰ :Experimental behavior of composite beam-column-connection [J]. Journal of Construction Steel Research.1994, 31(5):3-30.

[7]   Simoes da Silva L., Simoes R.D., Cruz P. Experimental behavior of end-plate beam-to-column composite joints under monotonical loading [J]. Engineering Structures. 2001, 23:1383-1409.

[8]   Shi W.L., Li G.Q., Xiao Y., Ye Z.M. Cyclic loading tests on composite beam-to-column joints with semi-rigid connections [J]. Journal of building structures. 2008, 29(5):57-66. (in Chinese)

[9]   Rong B., Chen Z.H., Zhang R.Y., Apostolos F., Yang N. Experimental and analytical investigation of the behavior of diaphragm-through joints of concrete-filled tubular columns. Journal of Mechanics of Materials and Structures. 2012, 7(10): 909-929.

[10]   Simoes da Silva L., Lima L.R.O., Vellasco P.C.G., Andrade S.A.L. Behaviour of flush end-plate beam-to-column joints under bending and axial force [J]. Steel Composite Structure. 2004, 4(2):77-94.

[11]   Del Savio A.A., Nethercot D.A., Vellasco P.C.G., Andrade S.A.L. Martha L.F. Generalised component-based model for beam-to-column connections including axial versus moment interaction [J]. Journal of Constructional Steel Research. 2009, 65:1876-1895.

[12]   Yang B., Tan K.H. Robustness of bolted-angle connections against progressive collapse: Mechanical modelling of bolted-angle connections under tension [J]. Engineering Structures. 2013, 57:153-168.

[13]   Yang B., Tan K.H. Robustness of bolted-angle connections against progressive collapse: Experimental tests of beam-column joints and development of component-based models. Journal of Structural Engineering, 2013, 139(9): 1498-1514.

[14]   Demonceau J.F., Jaspart J.P. Experimental test simulating a column loss in a composite frame. Advanced Steel Construction 2010, 6:891-913.

[15]   Guo L.H., Gao S., Wang Y.Y., Zhang S.M. Tests of rigid composite joints subjected to bending moment combined with tension [J]. Journal of Constructional Steel Research. 2014, 95:44-55.

[16]   Guo L.H., Gao S., Fu F., Wang Y.Y. Experimental study and numerical analysis of progressive collapse resistance of composite frame [J]. Journal of Constructional Steel Research. 2013, 89:236-251.

[17]   Guo L.H., Gao S., Fu F. Structural performance of semi-rigid composite frame under column loss [J]. Engineering Strucutres. 2015, 95:112-126.

[18] ABAQUS theory manual. Version 10.0.1 Hibbitt. Pawtucket (RI): Karlsson and Sorensen, Inc.; 2003.

[19] Zhang J., Zhang W.Y., Zhang Y.C. Study and execution of the multifunctional experimental facility [J]. Industrial construction, 2004, 34(3):40-43.(in Chinese)

[20] Gao Shan. Progressive collapse behavior of planar steel frame with composite beam [D]. China: Harbin Institute of Technology. 2014. (in Chinese)
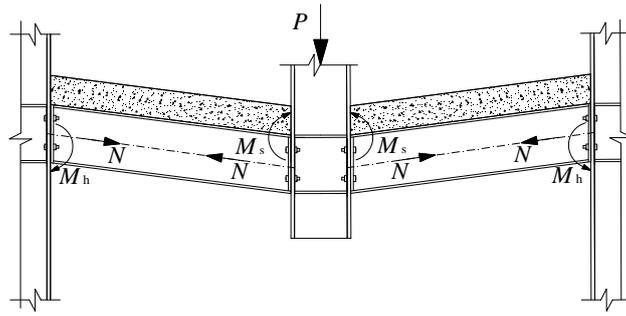
Fig. 1 Load-carrying mechanism transition
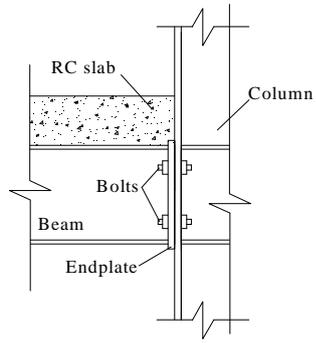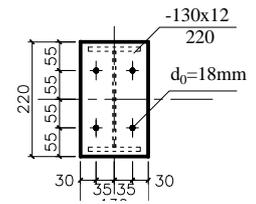
(a)flush endplate connection   (b)dimension of endplate

Fig. 2 Semi-rigid beam-to-column connection
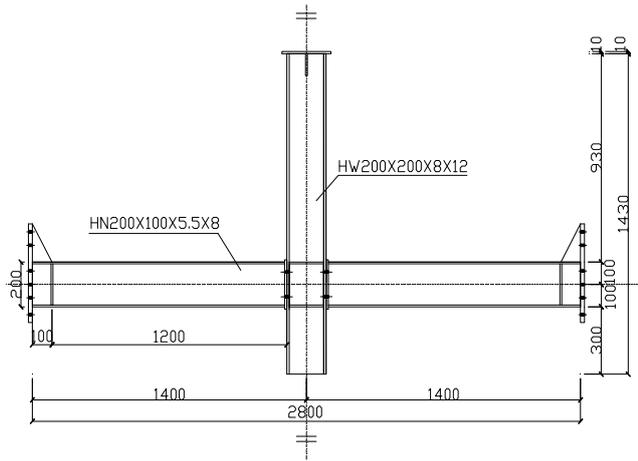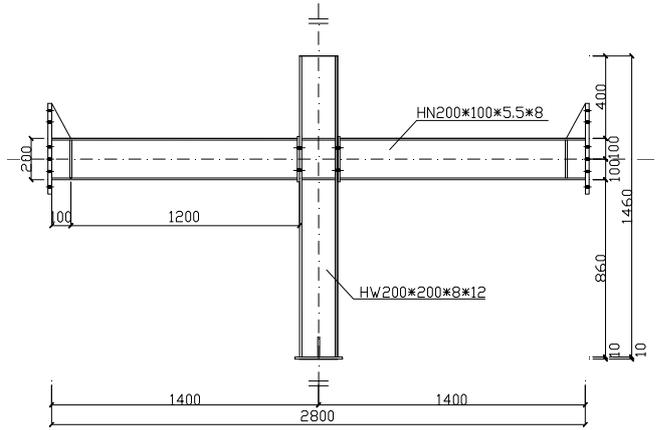
(a) SJS, SJST and SJST2　　　　　　　　　　　　　　(b) SJH, SJHT and SJT

Fig. 3 Dimension of steel specimens
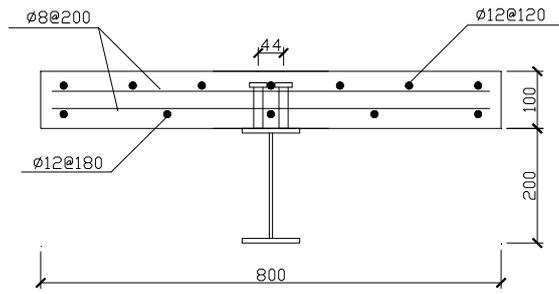
Fig. 4 Distribution of bars

Fig. 5 Multifunctional loading ring
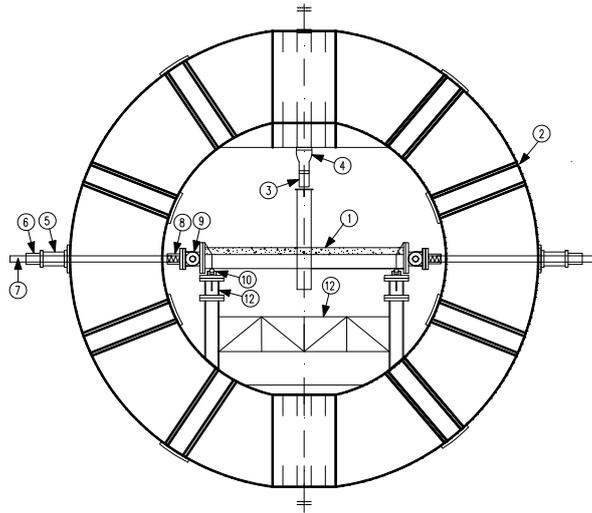
Fig. 6 Experimental setup:
① specimen; ② multifunctional loading ring; ③ load cell; ④ 500kN hydraulic jack;⑤2500kN hydraulic jack; ⑥load cell; ⑦ 90mm-diameter tension rod; ⑧bolt sleeve; ⑨connecting hinge; ⑩hinge support; ⑪support column; ⑫column bracing

(a) Step A (b) Step B
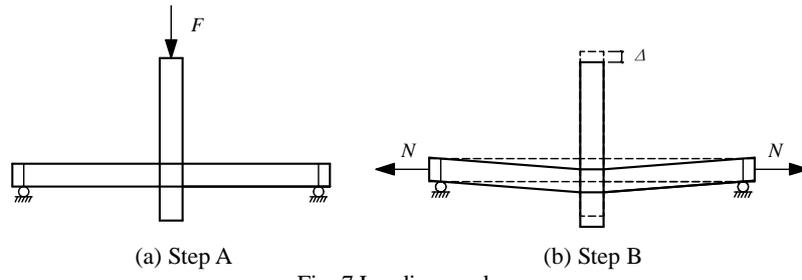
Fig. 7 Loading modes
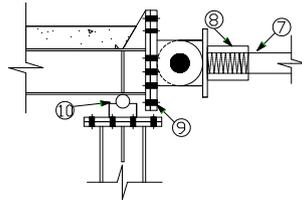
Fig. 8 Details of experimental setup
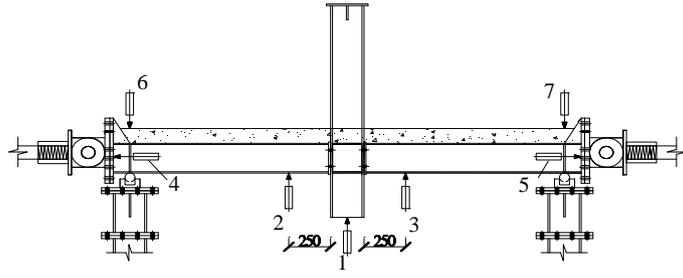
Fig. 9 Distribution of LVDT

(a)First crack on slab   (b) Crush at top of slab   (c) Bending of endplate   (d) Cracking pattern at top of slab
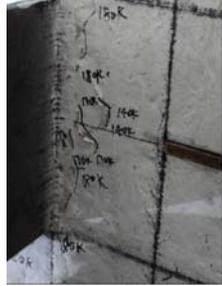
Fig. 10 Phenomenon of SJS
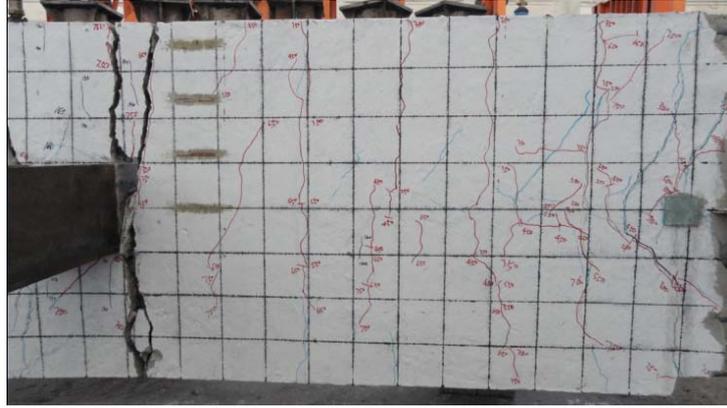
| (a)Endplate bending | (b)Cracking pattern at top of slab | (c)Fracture of welding seam |

Fig. 11 Phenomenon of SJST

(a)Cracking pattern at top of slab   (b)Fracture of welding seam
Fig. 12 Cracking pattern at slab top of SJST2
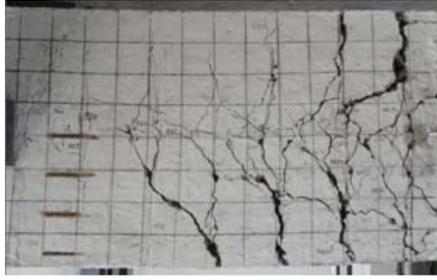
Fig. 13 Cracking pattern at the slab-top of the joint with rigid connections in Ref. [15]

(a)longitudinal cracks at top of slab

(b)Buckling of steel beam
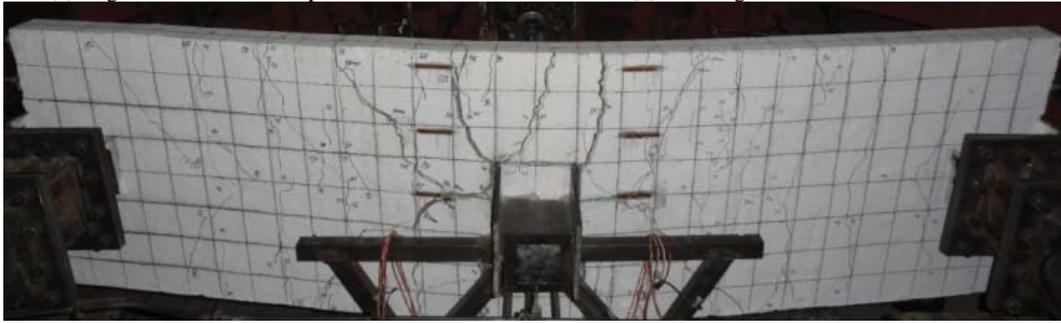
(c)cracking pattern at top of slab

Fig. 14 Phenomenon of SJH

(a)Fracture of welding seam

(b)Cracking pattern at top of slab

Fig. 15 Phenomenon of SJHT

(a)Deformation of the endplate   (b)Fracture of welding seam
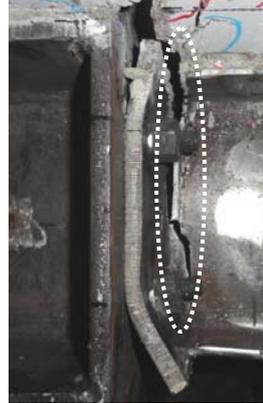
(c)Cracking pattern at top of slab
Fig. 16 Phenomenon of SJT
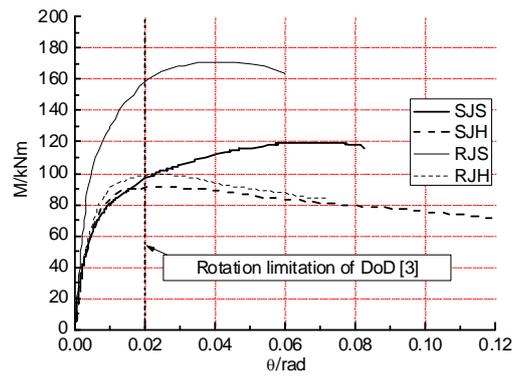
Fig. 17 Bending moment-rotation angle curves
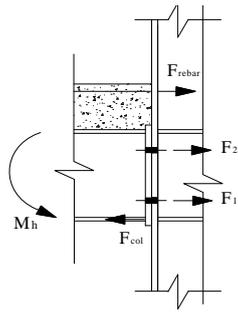
Fig. 18 Semi-rigid joints under hogging moment
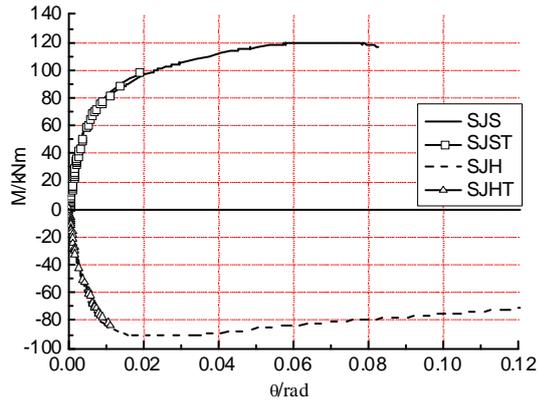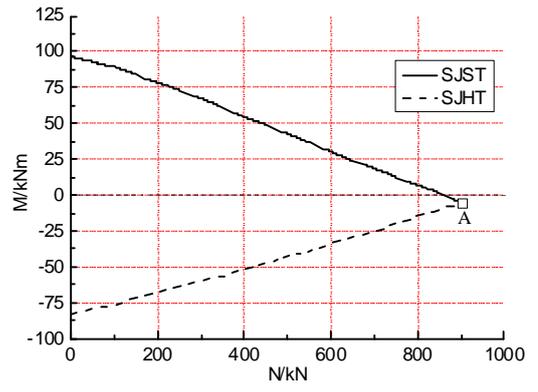
(a) Moment-rotation curves   (b) Moment-tensile force curves

Fig. 19 Experimental results of specimen SJST and specimen SJHT
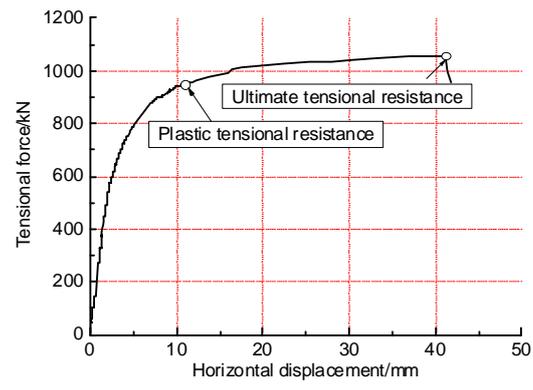
Fig. 20 Tensile force-horizontal displacement curve of specimen SJT
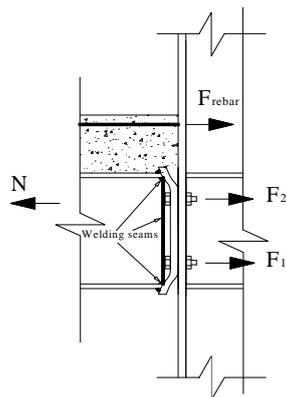
Fig. 21 Deformation of flush endplate under tensile
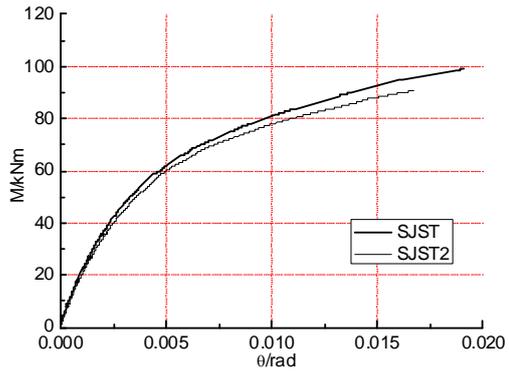
(a) Moment-rotation curves in step A   (b) Moment-tensile load curves in step B
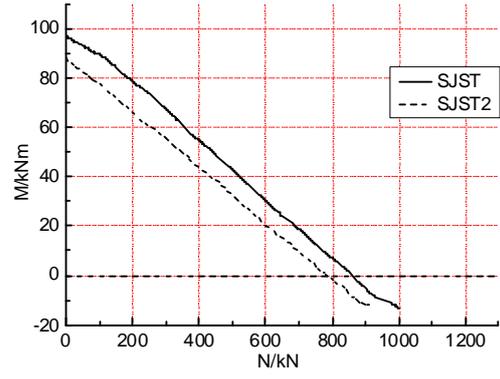
Fig. 22 Influence of bolt strength
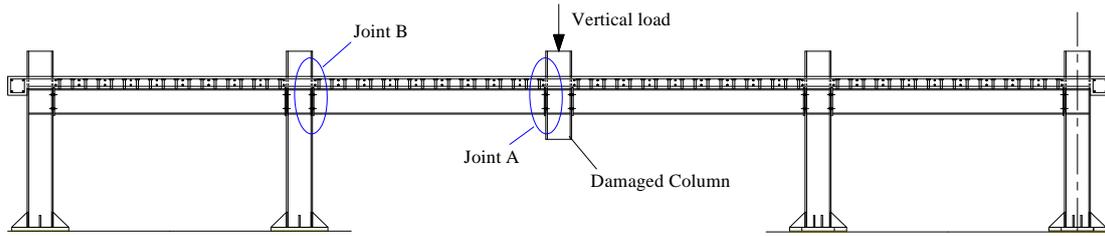
(a) Semi-rigid composite frame under middle column loss
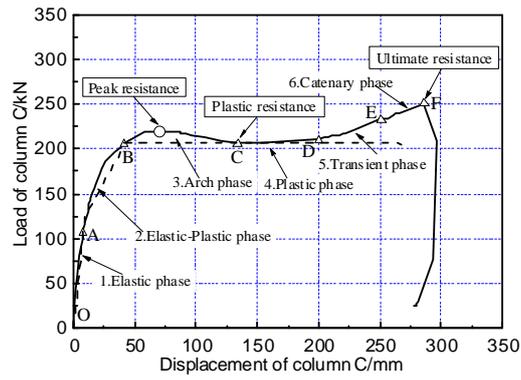
(b) Vertical load-displacement of middle column relationship curve

Fig. 23 Test of semi-rigid composite frame under column loss [17]
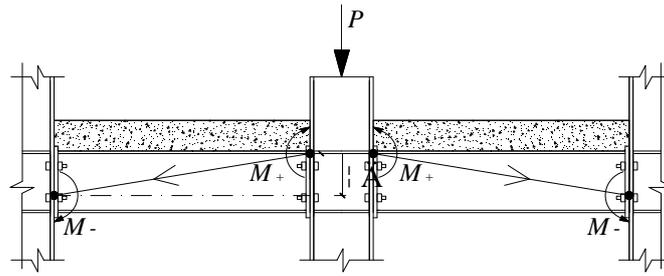
Fig. 24 Compressive arch action
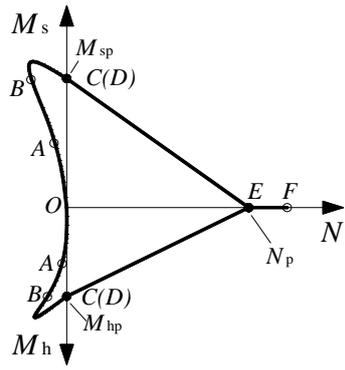
Fig. 25 Relationship curve between *M*
and *N* in the joint
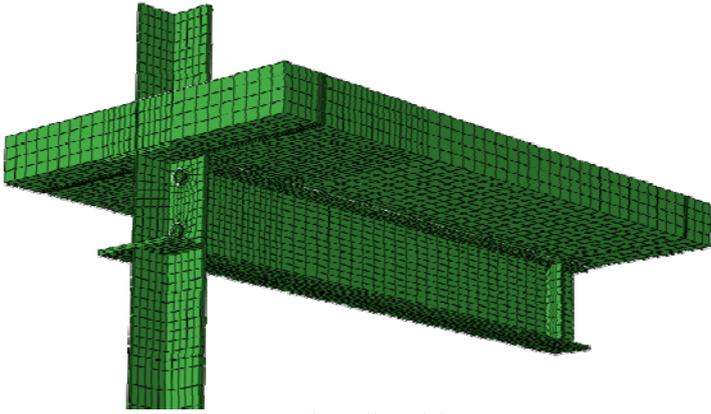
(a) Overall model
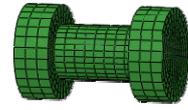
(b) High-strength Bolt

Fig. 26 Finite element model
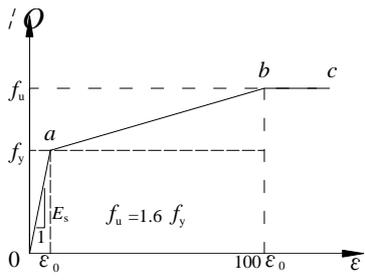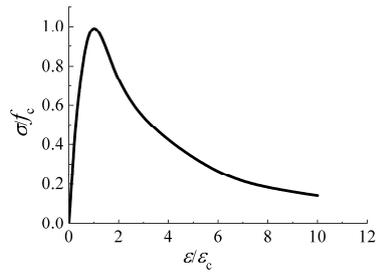
(a) Steel (b) Concrete in compression (c) Concrete in tension
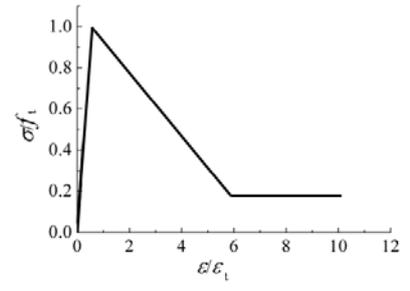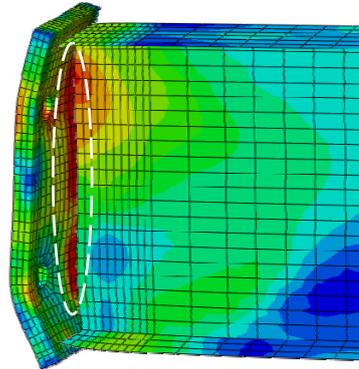
Fig. 27 Stress-strain relationship
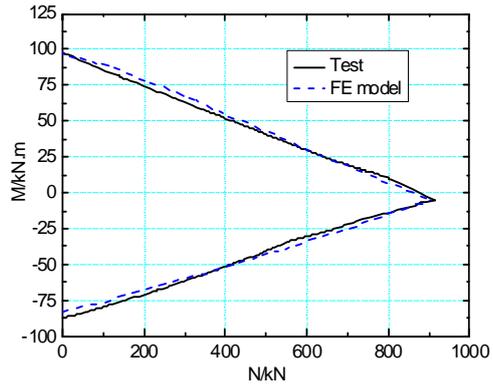
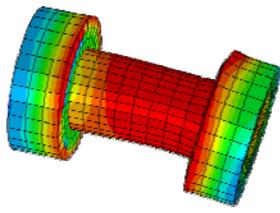Fig. 28 Validation of FE model
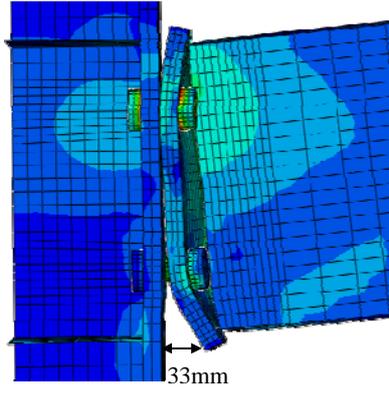
(a) FE model

(b) specimen SJT
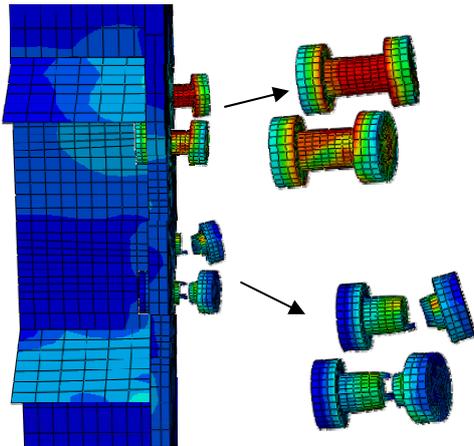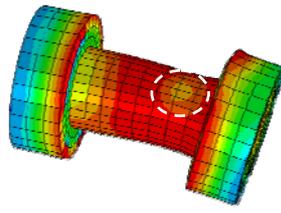
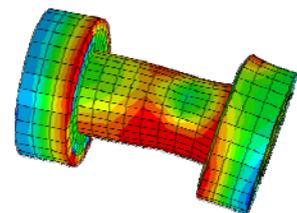(c) Fracture of bolts

(d) Von Mises stress of steel beam

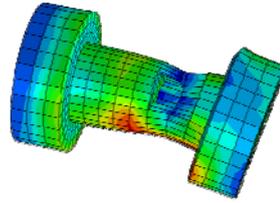Fig. 29 Deformation of the joint under tensile load
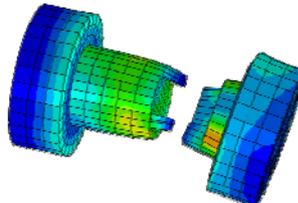
(a) Before fracture (b) Strength degradation initiated (c) Strength degradation progressed

(d) Fracture initiated (e) Bolt fractured (f) Fractured bolt in specimen SJST
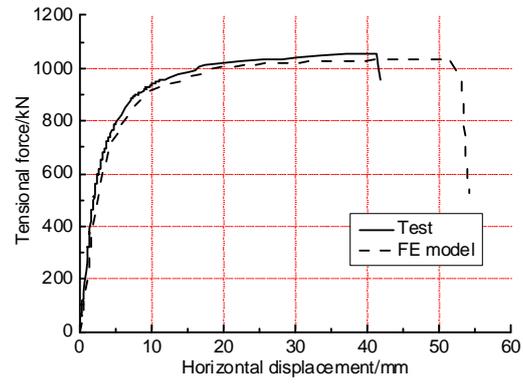
Fig. 30 Development of bolt fracture

Fig. 31 Validation of the   model with bolt fracture

Table 1 Design parameter of specimens

Specimen	Column	Beam	Slab /mm Thickness	Slab /mm Width	Rebar ratio	Loading condition
SJS						Sagging moment
SJST,SJST2						Sagging moment + Tensile force
SJH	HW200×200×8×12	HN200×100×5.5×8	100	800	0.85%	Hogging moment
SJHT						Hogging moment + Tensile force
SJT						Tensile force

Table 2 Mechanical properties of steel

Se.		f_y（MPa）	f_u（MPa）	E_s（10^5MPa）
Beam	Flange	269	401	1.96
	Web	275	411	2.09
Column	Flange	247	396	2.00
	Web	276	415	1.98
Bolt	10.9M	1089	1210	2.06
	8.8M	798	998	2.06
Reinforcement	Φ8	325	487	-
	Φ12	331	464	1.95

Table 3 Failure mode

Specimen	Failure mode
SJS (under sagging moment)	Bolt fracture
SJH (under hogging moment)	Welding seam fracture
SJST/SJST2 (under sagging moment and tensile force)	Bolt fracture and welding seam fracture
SJHT (under hogging moment and tensile force)	Welding seam fracture
SJT (under tensile force)	Welding seam fracture